# Monomer-to-Micelle Transition of Dihexanoylphosphatidylcholine: $^{13}C$ NMR and Raman Studies

**Ramon A. Burns, Jr.,[1a] Mary F. Roberts,*[1a] Richard Dluhy,[1b] and Richard Mendelsohn[1b]**

*Contribution from the Departments of Chemistry, Massachusetts Institute of Technology, Cambridge, Massachusetts 02139, and Rutgers University, Newark, New Jersey 07102.*
*Received January 28, 1981*

**Abstract:** The monomer-to-micelle transition of dihexanoylphosphatidylcholine has been studied by $^{13}C$ NMR and Raman spectroscopy. Lipid $^{13}C$ chemical shifts in a variety of solvents indicate that micellization chemical shift differences for many carbons can be successfully modeled as a simple transfer from a strong hydrogen bond donating solvent (methanol, $CHCl_3$) to a hydrogen bond donor deficient/acceptor solvent ($CCl_4$, THF, dioxane). This solvent transfer model fails to predict the micellization shift trends at three points in the lipid molecule: the acyl chain peaks, the carbonyls, and the glyceryl backbone methine carbon. The temperature dependence of the phospholipid $^{13}C$ chemical shifts suggests that the acyl chain micellization shifts are due to conformational changes through the $\gamma$ effect. This implies a 5% or 7% increase in $P_t$, the probability of a trans conformer in the acyl chain, for micellar vs. monomer lipid. A comparison of the micellization shifts of acyl chain carbons in dihexanoylphosphatidylcholine and its ether-linked analogue *rac*-dihexylphosphatidylcholine suggests similar small ordering effects in both micelles. Solvent transfer and the $\gamma$ effect cannot account for the $^{13}C$ micellization chemical shifts of the carbonyl and glyceryl backbone methine carbons. Therefore, a possible source of these shift discrepancies is a conformational change in the glyceryl backbone between monomer and micelle. Two regions of the Raman spectrum of dihexanoyl-PC micelles, namely the C–H and C–C stretching regions, are used to obtain independent structural information about the acyl chains. Data from the C–H stretching regions suggest that lateral interactions between the chains in the micelle are disrupted compared to ordered forms that occur at low temperature, thereby leading to reduced intensity for spectral features which depend on interchain interaction for their intensity. In addition, both the C–H and C–C stretching regions indicate the existence of substantial disorder in the hydrocarbon chain conformation. Comparison of the monomer and micelle spectra suggests that a slight increase in chain order may occur upon micelle formation. Thus, both techniques are consistent with the following changes in short-chain lecithin molecules upon micellization: the acyl chains become very slightly ordered and are in a less polar environment; at most only minor conformational changes occur in the glycerol backbone. This view of the monomer-to-micelle transition is discussed in relation to the interfacial activation of soluble phospholipases.

The synthetic short-chain lecithin dihexanoyl-PC[2] is an interesting substrate for a variety of phospholipases.[3] This double-chain amphiphile has a moderately high cmc (14 mM), and is a relatively poor substrate below this concentration.[4] Upon micellization, the enzymatic hydrolysis increases dramatically. Previous $^{13}C$ NMR studies have demonstrated changes in the lipid molecule such that differences in *sn*-1 and *sn*-2 acyl chains are accentuated in the micelle.[5] In order to assess possible lecithin conformational changes in relation to interfacial activation of phospholipases, we have obtained $^{13}C$ NMR spectra of aqueous dihexanoyl-PC as a function of lecithin concentration. Because all carbons are resolved, information is gained for all sections of the molecule. The acyl chain $^{13}C$ resonances shift downfield upon aggregation with a maximum of 0.6 ppm for the $\gamma$-methylene carbon. Carbonyl resonances move upfield more than 3 ppm upon micellization. Glycerol backbone resonances move upfield or downfield, and head-group resonances show little sensitivity to the transition.

Before detailed and useful information can be extracted from $^{13}C$ shift data, the relative contributions from solvent effects,[6] conformational effects,[7] electric field effects,[8] and a variety of other possible shift mechanisms must be determined. This can be done by examining the effects of a variety of solvents and temperature on $^{13}C$ chemical shifts of the lecithin.

By studying the monomer/micelle transition of this phospholipid with another technique with different sensitivities to factors such as solvent and conformation we can generate a self-consistent picture of the differences in conformation and motion between monomeric and micellar lipid. Raman spectroscopy is the appropriate complement to NMR because chain vibrations are sensitive to conformation and order and less sensitive to solvent changes.

In the present study, the Raman and $^{13}C$ chemical shift temperature dependences of lipids and model compounds demonstrate that the lipid chains remain remarkably fluid in the micelle, although minor chain constraints occur near the ester groups. Micellization decreases solvent polarity for head-group and backbone atoms and chain terminal methyl groups. A conformational change in the region of the glyceryl methine may also occur. This view of the monomer/micelle transition is useful in interpreting the interfacial activation of soluble phospholipases.

## Experimental Section

Dihexanoyl-PC and dibutyryl-PC were obtained from Calbiochem. Dioctanoyl-PC was synthesized as described previously.[5] Phospholipid purity was monitored by thin-layer chromatography.[5] Model compounds were the best grade commercially available. *rac*-Dihexyl-PC was synthesized by Mr. Jonathan Friedman, M.I.T.[9]

$^{13}C$ NMR spectra were obtained at 67.9 MHz with a Bruker 270 spectrometer. Samples contained 3–124 mM Lecithin in 10 mM potassium phosphate, 1 mM EDTA, in $D_2O$, pD 7.4. Chemical shifts in aqueous solutions are referenced with respect to [2-$^{13}C$]acetate (Kor Isotopes). Unless otherwise indicated, spectra were obtained at 30° C. Phosphate analyses were done for each spectrum to insure an accurate micellization curve based on lecithin concentration.[10] Specific details for referencing solvent and temperature $^{13}C$ chemical shift studies are given in the Results section.

(1) (a) Massachusetts Institute of Technology. (b) Rutgers University.
(2) The abbreviations and symbols are: diacyl-PC, 1,2-diacyl-*sn*-glycero-3-phosphorylcholine; $\alpha$, $\beta$, $\gamma$, $\omega - 1$, $\omega$, acyl chain carbons number 2 through 6 from the ester linkage.
(3) (a) DeHaas, G. H.; Bonsen, P. P. M.; Pieterson, W. A.; Van Deenen, L. L. M. *Biochim. Biophys. Acta* **1971**, *239*, 252. (b) Little, C. *Acta Chem. Scand., Ser. B*, **1977**, *B31*, 267.
(4) Wells, M. A. *Biochemistry* **1974**, *13*, 2248.
(5) Burns, R. A., Jr.; Roberts, M. F. *Biochemistry* **1980**, *19*, 3100.
(6) (a) Lichter, R. L.; Roberts, J. D. *J. Phys. Chem.* **1970**, *74*, 912. (b) Bacon, M. R.; Maciel, G. E. *J. Am. Chem. Soc.* **1973**, *95*, 2413.
(7) (a) Paul, E. G.; Grant, D. M. *J. Am. Chem. Soc.* **1963**, *85*, 1701. (b) Grant, D. M.; Cheney, B. V. *Ibid.* **1967**, *89*, 5315.
(8) Seidman, K.; Maciel, G. E. *J. Am. Chem. Soc.* **1977**, *99*, 3254.
(9) Burns, R. A., Jr.; Friedman, J. M.; Roberts, M. F. *Biochemistry* **1981**, *20*, 5945.
(10) Eaton, B. R.; Dennis, E. A. *Arch. Biochem. Biophys.* **1976**, *176*, 604.

0002-7863/82/1504-0430$01.25/0 

Table I. $^{13}C$ NMR Chemical Shifts (ppm from internal [2-$^{13}C$]Acetate) for Monomeric and Micellar Dihexanoyl-PC and Micellization Shifts for *rac*-Dihexyl-PC

| carbon atom | dihexanoyl-PC δ monomer | dihexanoyl-PC δ micelle | dihexanoyl-PC Δ[a] | dihexyl-PC Δ[b] |
|---|---|---|---|---|
| head group | | | | |
| $\overset{+}{N}(CH_3)_3$ | 30.73 | 30.73 | 0.00 | 0.02 |
| $CH_2N$ | 42.75 | 42.75 | 0.00 | −0.02 |
| $CH_2OP$ | 36.24 | 36.16 | −0.08 | −0.06 |
| backbone | | | | |
| $CH_2OP$ | 40.62 | 40.39 | −0.23 | −0.08 |
| CHO | 47.54 | 47.33 | −0.21 | 0.65 |
| $CH_2O$ | 39.35 | 39.68 | 0.33 | −0.02 |
| alkyl | | | | |
| 1 (*sn*-1) | 154.65 | 150.76 | −3.89 | −0.19, 1.02[c] |
| (*sn*-2) | 154.07 | | −3.31 | |
| 2 (*sn*-1) | 10.49 | 10.55 | 0.06 | 0.56, .83 |
| (*sn*-2) | 10.68 | 10.64 | −0.04 | |
| 3 (*sn*-1) | 0.77 | 1.01 | 0.24 | 0.68, .59 |
| (*sn*-2) | | 1.12 | 0.35 | |
| 4 (*sn*-1) | 7.21 | 7.82 | 0.61 | 0.62 |
| (*sn*-2) | | 7.68 | 0.47 | |
| 5 | −1.63 | −1.18 | 0.45 | 0.50 |
| 6 | −10.06 | −9.77 | 0.29 | 0.42 |

[a] Micellization shifts determined as described in Results. [b] Micellization shifts from ref 9; the cmc of this lipid is 8 mM. [c] The first peak in each pair is the most downfield peak; *sn*-1/*sn*-2 identifications have not been unambiguously determined for this ether-linked lipid.

The Raman apparatus consists of a Jarrell-Ash $^3/_4$-m double monochromator, Spectra-Physics Model 164 $Ar^+$ laser, and RCA C31034 photomultiplier. Photon counting detection is accomplished with a Spex Industries DPC-2 counter. The output from the photon counter is fed into a Spex Industries "Scamp" minicomputer, which controls the data acquisition and reduction. Typical spectral conditions used were: excitation frequency 5145 Å; Laser power 300 mW; residence time 0.5 s/cm$^{-1}$; number of scans 5–10; resolution 6 cm$^{-1}$; frequencies calibrated using atomic emission lines from a Neon lamp. Frequency accuracy is estimated at ±1–2 cm$^{-1}$ for sharp features.

## Results

**$^{13}C$ Chemical Shifts of Monomer/Micelle Dihexanoyl-PC and *rac*-Dihexyl-PC.** Representative curves showing the behavior of $^{13}C$ chemical shifts as a function of lecithin concentration are shown in Figure 1. For each carbon in the molecule the monomer $^{13}C$ chemical shift was determined by averaging the nearly constant values below the cmc (Table I). The micellar shifts in Table I were obtained from a linear least-squares fit of inverse chemical shift vs. lipid concentration as described elsewhere.[11] These fits used ≥9 points and had coefficients of determination ≥0.98. By using these limiting shifts, the seven peaks showing the largest monomer/micelle shift change (excluding the carbonyls) were fit to an equilibrium constant model for micellization.[12]

$$K_{eq} = (X_n)^{1/n}/(X_1)$$

In this equation, $X_n$ is the concentration of micelles, $X_1$ is the monomer concentration, and $n$ is the number of monomers per micelle. The value $n = 32$ was used in this calculation, in agreement with light-scattering studies of the dihexanoyl-PC micelles.[13] A value of $\Delta G_{mic} = -RT \ln K_{eq} = -2.6$ (±0.1) kcal/mol (per mole of monomer) was obtained. A cmc of approximately 14 mM was obtained from this analysis in good agreement with results from other studies.[13-15] These parameters were used to calculate the titration curves shown in Figure 1. No evidence is seen for more than one micelle transition as was suggested by Allgyer and Wells.[16]

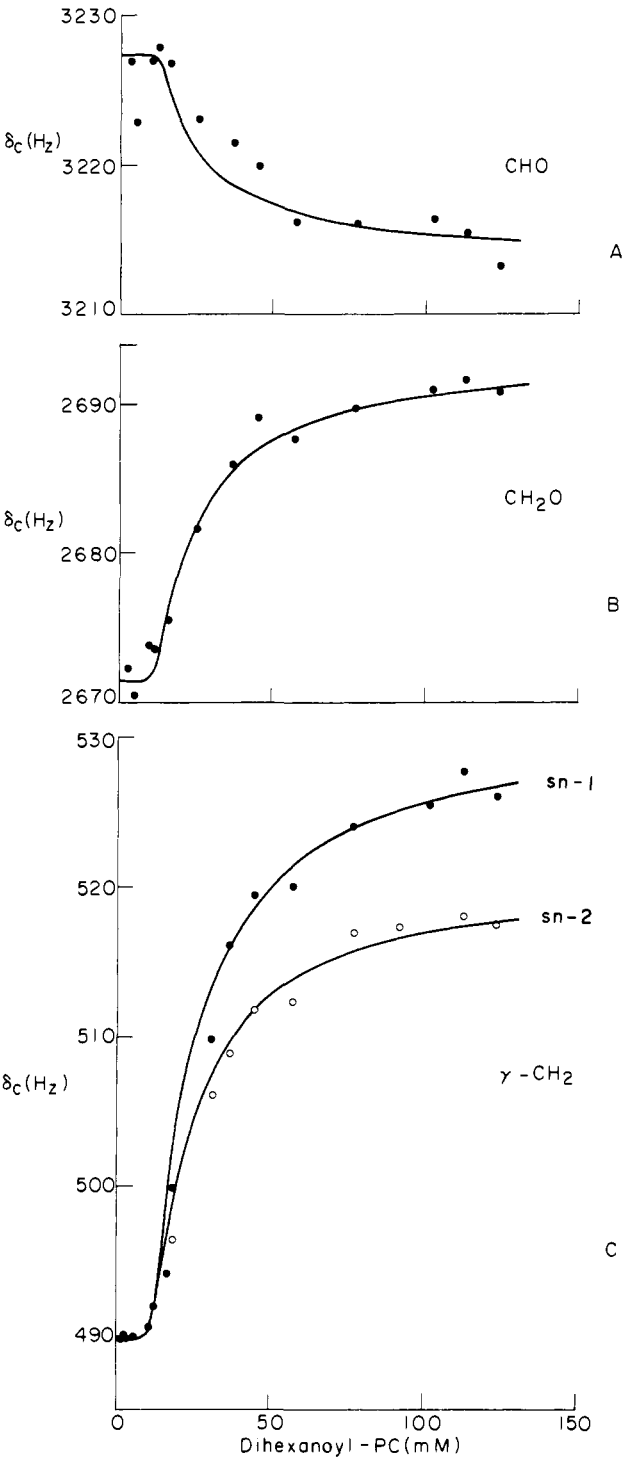


Figure 1. $^{13}C$ chemical shifts (ppm from [2-$^{13}C$]acetate) of selected carbons of dihexanoyl-PC as a function of lecithin concentration: (A) glyceryl CHO; (B) glyceryl $CH_2O$; (C) acyl chain γ-$CH_2$ group.

$^{13}C$ spectra of the acyl chain region for monomeric and micellar dihexanoyl-PC are shown in Figure 2. The acyl chain carbon atoms shift downfield upon micellization, although carbon number

(11) Persson, B.-O.; Drakenberg, T.; Lindman, B. *J. Phys. Chem.* **1976**, *80*, 2124.
(12) Tanford, C. "The Hydrophobic Effect", 2nd ed.; Wiley-Interscience: New York, 1980; p 63.
(13) (a) Tausk, R. J. M.; Karmiggelt, J.; Oudshoorn, C.; Overbeek, J. Th. G. *Biophys. Chem.* **1974**, *1*, 175. (b) Quasielastic light-scattering studies of the dihexanoyl-PC micelles indicate no significant changes in micelle size within the concentration range of this study (Missel, P.; Burns, R. A., Jr.; Roberts, M. F.; Benedek, G. B., unpublished results).
(14) Hershberg, R. D.; Reed, G. H.; Slotboom, A. J.; DeHaas, G. H. *Biochim. Biophys. Acta* **1976**, *424*, 73.
(15) Schmidt, C. F.; Barenholz, Y.; Huang, C.; Thompson, T. E. *Biochemistry* **1977**, *16*, 3948.
(16) Allgyer, T. T.; Wells, M. A. *Biochemistry* **1979**, *18*, 4354.

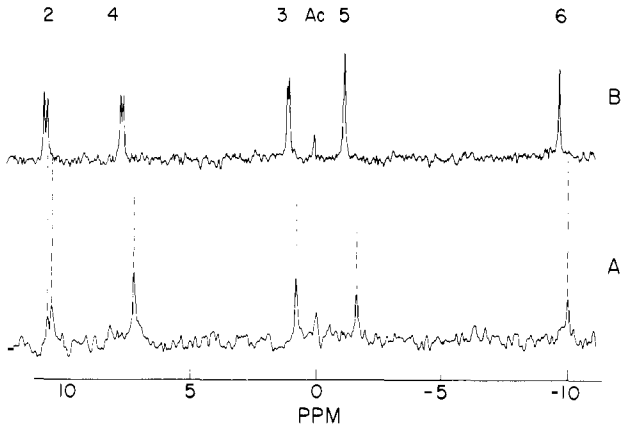


**Figure 2.** $^{13}C$ NMR spectra of the acyl chain region of (A) monomeric (4 mM) and (B) micellar (57 mM) dihexanoyl-PC. Peak identifications are shown.

Table II. Solvent Effects of $^{13}C$ NMR Chemical Shifts of Dihexanoyl-PC

| carbon atom | I av absolute solvent diff,[a] ppm | II $\delta_{nonpolar} - \delta_{polar}$,[b] ppm | III well-behaved $\delta_{nonpolar} - \delta_{polar}$,[c] ppm |
|---|---|---|---|
| head group | | | |
| $N(CH_3)_3$ | 0.3 (0.2)[d] | −0.2 (0.3) | 0.01 (0.07) |
| $CH_2N$ | 0.3 (0.3) | 0.2 (0.5) | 0.12 (0.33) |
| $CH_2OP$ | 0.3 (0.2) | −0.1 (0.3) | −0.12 (0.18) |
| backbone | | | |
| $CH_2OP$ | 0.5 (0.3) | −0.7 (0.2) | −0.45 (0.16) |
| CHO | 0.4 (0.3) | 0.6 (0.1) | 0.34 (0.08) |
| $CH_2O$ | 0.4 (0.3) | 0.6 (0.3) | 0.46 (0.16) |
| carbonyl | 0.4 (0.3) | −0.8 (0.2) | −0.53 (0.14) |
| alkyl chains | | | |
| 2 | 0.2 (0.1) | 0.0 (0.2) | 0.10 (0.07) |
| 3 | 0.1 (0.1) | 0.0 (0.1) | 0.04 (0.06) |
| 4 | 0.1 (0.1) | 0.1 (0.1) | 0.06 (0.04) |
| 5 | 0.1 (0.1) | 0.15 (0.1) | 0.08 (0.06) |
| 6 | 0.3 (0.2) | 0.4 (0.3) | 0.37 (0.11) |

[a] The average absolute value for all possible solvent differences generated with a ten-solvent data base. [b] A subset of the entire data base using 11 solvent pairs which generate the largest carbonyl shifts in a polar-to-nonpolar transition. [c] Based on solvent pairs of $CH_3OH$, $CCl_4$, THF, dioxane, DMF, and benzene (i.e., excluding $CHCl_3$, $CH_2Cl_2$, $CH_3CN$, and pyridine). [d] Numbers in parentheses indicate standard deviations.

2 in both chains is relatively insensitive to the transition. The micellization shifts as a function of chain carbon atom are shown in Figure 3A. The largest change observed in the acyl chains is the 0.61 ppm downfield shift for carbon number 4 in the *sn*-1 chain. The glyceryl backbone $CH_2O$ for the *sn*-1 chain shows a significant downfield shift, while the remaining two carbon atoms in the backbone show significant upfield changes in shift upon micellization. Head-group carbon atoms show little or no sensitivity to the monomer/micelle transition. The carbonyl chemical shifts show extremely large upfield shifts upon micellization, as noted previously,[15] although the changes observed in this study are 1.5 to 2 times larger than in the earlier study. This difference probably reflects the fact that the carbonyl shift is pH dependent, and solutions not adequately buffered can give erroneous limiting shifts.

Chemical shift differences for the monomer/micelle transition of dihexyl-PC show slightly different characteristics from those of dihexanoyl-PC. The most prominent differences lie within three chemical bonds of the carbonyl/methylene substitution site, the backbone CHO, and acyl chain carbons 1 and 2 and to a lesser extent 3. These differences could be based on conformational characteristics or shift mechanisms determined by the presence (or absence) of the carbonyl moiety. Interestingly, the proximity

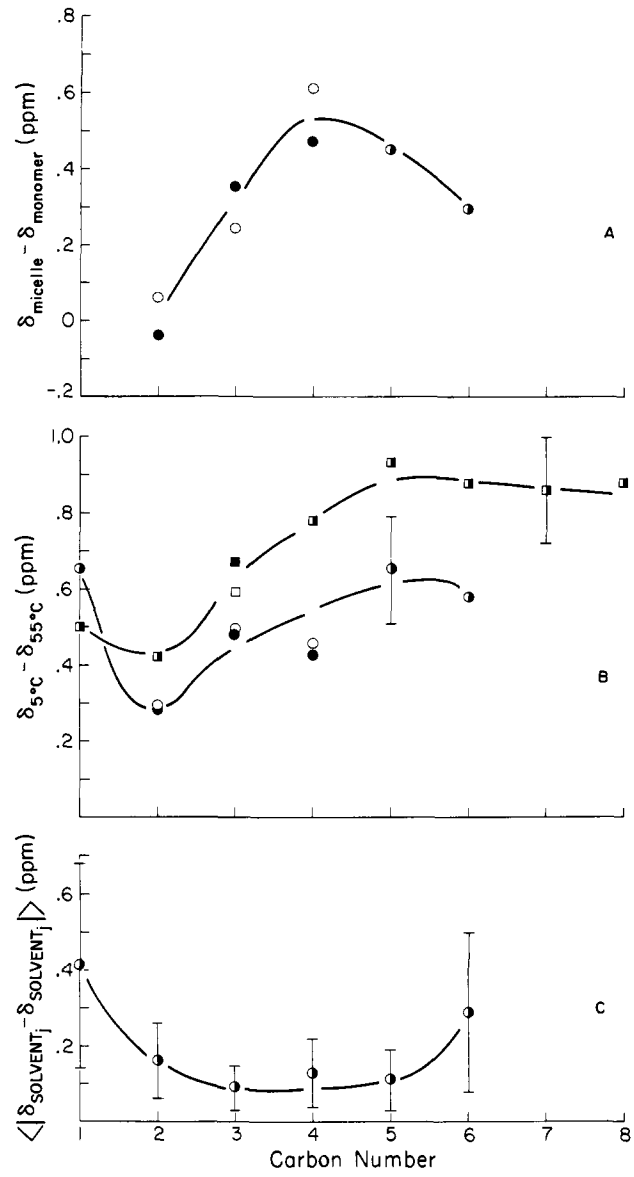


**Figure 3.** Changes in $^{13}C$ chemical shift behavior of short-chain lecithin acyl chains as a function of carbon number. (A) Micellization shifts for dihexanoyl-PC: (●) denotes *sn*-2 carbon atoms, (○) denotes *sn*-1 carbon atoms, (◑) denotes carbon atoms where the two chains are magnetically equivalent. (B) Relative temperature shifts for dihexanoyl-PC (circles) and dioctanoyl-PC (squares): open symbols denote *sn*-1 carbons, filled symbols denote *sn*-2 carbon atoms, and half-filled symbols denote nondifferentiated chain positions. Typical uncertainties are shown. (C) The average absolute solvent chemical shift difference (as defined in the text) for acyl chain carbons of dihexanoyl-PC; bars indicate standard deviations for each position.

of these sites to the carbonyl are appropriate for carbonyl-generated electric-field effects at saturated carbon centers.[6b] Micellization shifts for carbons 4–6 are very similar in both compounds, although they are consistently larger for the ether-linked compound.

**Solvent Effects on $^{13}C$ Chemical Shifts.** Dihexanoyl-PC $^{13}C$ chemical shifts were examined in ten different solvents with $Me_4Si$ as the internal standard. Shift changes between lipid and $Me_4Si$ contain chemical shielding changes for carbon atoms in both molecules. The $Me_4Si$ chemical shift depends on the solvent.[6b] Therefore, all dihexanoyl-PC shifts are corrected for the reported solvent dependence of $Me_4Si$. Using the ten-solvent data base, we can generate the average absolute value for all possible solvent differences (Table II). This is shown for acyl chain carbons in Figure 3C. These data indicate the relative sensitivity of lecithin carbons to solvent effects: backbone, head-group, carbonyl, and terminal methyl peaks have a larger solvent variability than acyl

chain methylene resonances. Within the acyl chain, the terminal methyl and $\alpha$-methylene carbons are more solvent dependent than chain carbons 3–5.

Column 2 of Table II shows the average shift changes for 11 of the 45 possible solvent pairs which generate the largest carbonyl solvent difference shift changes. These shift differences are averaged as $\delta_{nonpolar} - \delta_{polar}$, to correspond to $\delta_{mic} - \delta_{mon}$. These solvent pairs predict the characteristics of the monomer/micelle transition moderately well. However, within this set of solvent differences, two subsets of solvent-transfer characteristics are found. Shift data in $CHCl_3$, $CH_2Cl_2$, acetonitrile, or pyridine show a large solvent transfer chemical shift difference at the choline methyl, and a chemical shift gradient becoming more positive down the acyl chains. In contrast, solvent dependent shift differences using the solvents methanol, $CCl_4$, THF, dioxane, DMF, and benzene show small shift differences at the choline methyl groups and constant shift changes at acyl chain positions 3 through 5. Column 3 of Table II shows the results of averaging these five solvent pairs in the second ("well-behaved") set. In addition, these average solvent transfer shift changes have been divided by 1.61, so that the magnitude of the average solvent shift change and the monomer/micelle transition shift characteristics are similar. These solvent transfer shift changes predict the characteristics of the monomer/micelle transition with reasonable accuracy: small shift changes are observed in the head group, upfield shift at the glyceryl $CH_2OP$, downfield at $CH_2O$, etc. However, the upfield shift observed for the backbone CHO is completely anomalous. Even within the larger eleven-solvent-pair data base, an upfield shift is never observed at this carbon atom. (The CHO shift for diheptyl-PC is downfield, in agreement with the solvent pair data.) No solvent pair in this larger data base predicts the large upfield carbonyl shifts upon micellization, although the correct shift direction is predicted. Also, the magnitude of the downfield acyl chain chemical shifts is underestimated and the profile different in shape from that observed in the monomer/micelle transition.

Within the eleven pair solvent data base monomeric dihexanoyl-PC is modeled by highly hydrogen-bond-donating solvents; micelles are modeled by H-bond donor deficient or H-bond accepting solvents. The dominant shift mechanism for head-group and backbone carbon atoms in the monomer/micelle transition is apparently a loss of H-bond-donating water molecules for micellar lipid. All carbon atoms in the backbone and head group are directly bonded to heteroatoms; interactions between solvent and lipid heteroatoms could be the source for the observed shift changes. The small shift changes observed upon micellization for the head-group carbon atoms are correctly predicted by the solvent transfer model. Thus, the lack of large shift changes in the head group does not simply indicate that the head-group environment is the same for monomeric and micellar lipid. The solvent transfer data demonstrate that head-group chemical shifts are not expected to change, i.e., the choline head group carbon atom chemical shifts are not sensitive to changes in proton-donating ability of the solvent.

In contrast, the $^{13}C$ chemical shift changes for the monomer/micelle transition are larger for acyl-chain than backbone or head-group peaks. Furthermore, the micellization shift pattern observed for the acyl-chain carbons is in conflict with the solvent studies (Figure 3A,C): upon micellization chain carbons 3, 4, and 5 shift the most while the terminal methyl and C-2 shift the least. In this region of the molecule, something more than solvent effects is responsible for the chemical shift changes upon aggregation.

**Temperature Dependence of the $^{13}C$ Chemical Shifts.** The temperature dependence of $^{13}C$ chemical shifts has been used to investigate the conformation of a variety of polymers,[17] hydrocarbons,[18] and lipids.[19] Interpretation of the observed shift changes is based on the "$\gamma$ effect".[7b,20] The introduction of a gauche conformation in an otherwise all-trans chain will bring carbon atom $n + 4$ into close proximity to carbon atom $n$. This shields carbon atom $n$, moving its resonance position upfield. Several studies[17b,18a,20,21] suggest 5 ppm as the shift difference between the trans and gauche conformers of saturated alkyl chains. If the acyl chains are in a more trans conformation in the micelle than as a monomer, then the $\gamma$ effect predicts that micellar carbons should be downfield of the corresponding monomer shifts. Therefore, the $\gamma$ effect predicts the chemical shift direction observed in the monomer/micelle transition.

Table III. Relative Temperature Coefficients of $^{13}C$ NMR Chemical Shifts (Hz/°C) for Short-Chain Lecithins

| carbon atom | micelle: dioctanoyl-PC ($D_2O$) | monomers: dioctanoyl-PC ($CD_3OD$) | monomers: dibutyryl-PC ($D_2O$) |
|---|---|---|---|
| head group | | | |
| $N(CH_3)_3$ | 0.0 (0.2)[a] | 0.0 (0.1) | 0.0 (0.1) |
| $CH_2N$ | 0.0 (0.2) | 0.2 (0.1) | −0.1 (0.1) |
| $CH_2OP$ | −0.4 (0.1) | −0.5 (0.1) | −0.3 (0.1) |
| backbone | | | |
| $CH_2OP$ | 0.0 (0.3) | −0.4 (0.1) | −0.1 (0.2) |
| CHO | −0.1 (0.2) | 0.0 (0.2) | 0.1 (0.2) |
| $CH_2O$ | −0.2 (0.2) | −0.3 (0.1) | −0.2 (0.1) |
| carbonyl | −0.5 (0.1) | −0.3 (0.1)<br>−0.4 (0.1) | −0.4 (0.6) |
| alkyl chains: | | | |
| 2 (*sn*-1) | −0.4 (0.1) | −0.3 (0.1) | −0.3 (0.2) |
| (*sn*-2) | | −0.3 (0.1) | |
| 3 (*sn*-1) | −0.6 (0.2) | −0.5 (0.1) | −0.3 (0.1) |
| (*sn*-2) | −0.7 (0.2) | | |
| 4 | −0.8 (0.2) | −0.7 (0.1) | −0.3 (0.1) |
| 5 | −0.9 (0.2) | | |
| 6 | −0.9 (0.1) | −0.7 (0.1) | |
| 7 | −0.9 (0.1) | −0.8 (0.1) | |
| 8 | −0.9 (0.2) | −0.8 (0.1) | |

[a] Numbers in parentheses reflect uncertainties in the fitting procedure outlined in the Results.

Studies of the temperature dependence of $^{13}C$ chemical shifts are complicated by specific solute–solvent interactions, chemical shift changes of reference compounds as a function of temperature, changes in shift due to greater excited state contribution to the chemical shift at high temperature, etc. Difficulties of this kind are indicated by a 6 and 40 Hz movement (relative to the lock frequency) of the reference $Me_4Si$ and [2-$^{13}C$]acetate across a 50 °C temperature change (data not shown). Indeed, the temperature dependence of the chemical shift for the $Me_4Si$ observed in this study does not exactly agree with that determined at a different field strength.[22] This makes interpretation of the absolute temperature coefficient problematical. To overcome this difficulty, we have defined the observed choline methyl shift as zero, and related all other temperature coefficients to this reference point. Since the choline methyl group chemical shift change for the monomer/micelle transition is also zero, direct comparison of these relative temperature coefficients to monomer/micelle shift changes if facilitated.

If phospholipid cmc values are temperature dependent, shift changes reflecting monomer/micelle populations could complicate the temperature studies. Therefore, the eight-carbon lecithin was also used in temperature studies because of its lower cmc (0.2 mM)[14a] compared to that of dihexanoyl-PC (14 mM). Relative temperature coefficients are shown in Table III for dioctanoyl-PC in $CD_3OD$ (where the lipid is monomeric) and in $D_2O$ (at sufficiently high concentrations to be essentially all micellar) and for dibutyryl-PC in $D_2O$. The latter lecithin has a very high cmc and is an aqueous monomer model.[5] For a given carbon atom these relative temperature coefficients are all very similar, re-

(17) (a) Randall, J. C. "Polymer Sequence Determination"; Academic Press: New York, 1977. (b) Tonelli, A. E.; Schilling, F. C.; Starner, W. H., Jr.; Sheperd, L.; Plitz, I. M. *Macromolecules*, **1979**, *12*, 78.
(18) (a) Tonelli, A. E. *Macromolecules* **1979**, *12*, 83. (b) Ritter, W.; Moller, M.; Cantow, H.-J. *Makromol. Chem.* **1978**, *179*, 823.
(19) Callaghan, P. T.; Jolley, K. W. *Chem. Phys. Lipids* **1979**, *23*, 133.
(20) Cheny, B. V.; Grant, D. M. *J. Am. Chem. Soc.* **1967**, *89*, 5319.
(21) Spiescke, H.; Schneider, W. G. *J. Chem. Phys.* **1961**, *35*, 722.
(22) Schneider, H. J.; Freitag, W.; Schommer, M. *J. Magn. Reson.* **1975**, *18*, 393.

Table IV. Raman Spectral Data for the C-H Stretching Region of Dihexanoyl-PC and Hexanoic Acid

| hexanoic acid | | dihexanoyl-PC | | | | | |
|---|---|---|---|---|---|---|---|
| | | | micelle | | $CDCl_3$ solution | | |
| liquid 22 °C | solid −47 °C | monomer 22 °C | in ice −25 °C | aqueous 22 °C | −100 °C | 22 °C | assignment |
| 2864 (sh) | 2856 (4) | 2865 (sh) | 2859 (sh) | 2864 (sh) | 2861 (5) | 2865 (sh) | $CH_2$ symmetric stretch |
| 2877 (9) | 2873 (8) | 2881 (3) | 2879 (8) | 2879 (7) | 2876 (7) | 2881 (6) | overtone of $CH_3$ deformation in Fermi resonance with $CH_3$ sym stretch |
| | 2902 (10) | | 2906 (9) | 2907 (sh) | 2903 (8) | | $CH_2$ antisym stretch |
| 2919 (9, br) | | 2920 (sh, br) | | 2920 (sh) | | 2921 (sh) | IR active $CH_2$ antisym stretch |
| | 2923 (8) | | 2923 (sh) | | | | $\alpha$-$CH_2$ antisym stretch |
| 2935 (10) | 2936 (6) | 2945 (10) | 2941 (10) | 2941 (10) | 2937 (10) | 2937 (10) | acyl chain methyl $CH_3$ sym stretch |
| 2960 (sh) | 2960 (5) | | 2967 (9) | | 2964 (9) | 2967 (6) | acyl chain methyl $CH_3$ asym stretch |
| | | 2974 (9) | | 2976 (7) | | | choline methyl stretching |
| | | | 2984 (sh) | 2985 (sh) | | 2985 (sh) | choline methyl stretching |

[a] Frequencies in $cm^{-1}$, intensities in parentheses with 10 arbitrarily assigned to the strongest feature in each spectrum: br = broad, sh = shoulder.

gardless of the physical state of the molecule (i.e., monomer or micelle). If molecular conformation controls the temperature dependence, then the relative temperature coefficients are determined by both the energy difference and chemical shift difference between (at least) two conformational states. A similar coefficient for a given carbon does not guarantee that molecular conformation is the same. However, with regard to the ability of this measurement to characterize conformational energetics, monomeric and micellar lecithins appear quite similar.

Inspection of Table III shows that the majority of head-group and backbone carbon atoms have a relative temperature coefficient around zero, i.e., similar to that of the choline methyl group. If monomeric and micellar relative temperature coefficients are averaged for any given carbon atom, only the choline $CH_2OP$ and the backbone $CH_2O$ appear to differ significantly from zero. With increasing temperature, carbonyl and acyl chain carbons move upfield more than the reference choline methyl group and the majority of backbone and head-group carbon atoms. If a simple trans, gauche (±) model is set up for the acyl chain methylene conformational states with an energy difference of 560 cal/mol between trans and gauche states[23] and a $\gamma$ effect of 5 ppm, then an absolute temperature coefficient of −0.3 Hz/K is calculated at the field strength used in this study. Both the direction and magnitude of the measured relative temperature coefficients support the $\gamma$ effect as an important chemical shift mechanism for the lipid temperature dependence. In order to facillitate comparison of acyl carbon micellization shifts with those caused by the $\gamma$ effect, Figure 3B shows the changes in carbon chemical shifts for micellar dioctanoyl-PC and dihexanoyl-PC observed upon decreasing the temperature from 55 to 5 °C. Both micellization and temperature-induced shift profiles are reasonably similar.

**Raman Spectroscopic Studies of Dihexanoyl-PC and Related Model Compounds.** Two regions of the Raman spectrum of phospholipids have been widely used to monitor conformational changes in the hydrocarbon chains.[24] The spectral region 2850–3000 $cm^{-1}$ contains the C–H stretching modes, for which assignments of spectral features and determination of spectra–structure correlations have been given by several authors.[25] Raman spectra for dihexanoyl-PC in aqueous micelle form, $CDCl_3$ solution, and aqueous monomer form are shown in Figures 4 and 5, while spectra of the model for the hydrocarbon chains, *n*-hexanoic acid in the solid and liquid states, are shown in Figure 6. Frequencies and assignments of spectral features are given in Table IV. The assignments are based on initial studies for

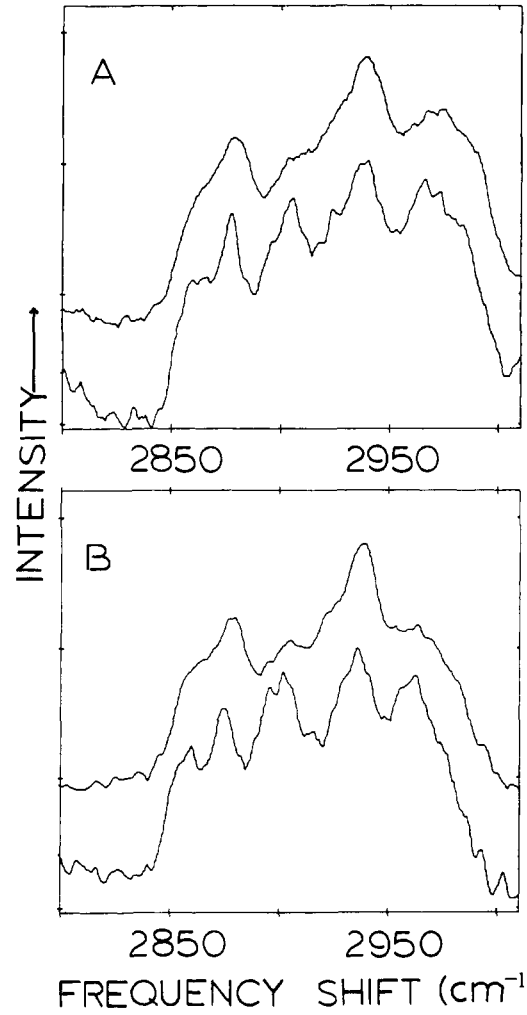


**Figure 4.** (A) Raman spectra of the C–H stretching region for (i, top) dihexanoyl-PC 168 mM in 1 mM EDTA, 50 mM Tris solution at 22 °C and (ii, bottom) dihexanoyl-PC as above except the temperature was −25 °C (micelle is frozen in ice). (B) Raman spectra of the C–H stretching region for (i, top) dihexanoyl-PC in $CDCl_3$ solution at −22 °C and (ii, bottom) dihexanoyl-PC as above except the temperature is −100 °C. Spectral conditions: parameters as in Experimental Section; data have been seven-point smoothed.

paraffin-related molecules,[26] as well as more recent work on the vibrational spectra of *n*-alkyl carboxylic acids.[27]

(23) Kint, S.; Scherer, J. R.; Snyder, R. G. *J. Chem. Phys.* **1980**, *73*, 2599.
(24) (a) Lord, R. C.; Mendelsohn, R. *Mol. Biol., Biochem. Biophys.* **1981**, *31*, 377. (b) Carey, P. R.; Salares, V. R. *Infrared Raman Spectrosc.* **1980**, *7*, 1.
(25) (a) Gaber, B. P.; Yager, P.; and Peticolas, W. L. *Biophys. J.* **1978**, *21*, 161. (b) Bunow, M. R.; Levin, I. W. *Biochim. Biophys. Acta* **1977**, *487*, 388. (c) Sunder, S.; Mendelsohn, R.; Bernstein, H. J. *Chem. Phys. Lipids* **1976**, *17*, 456.
(26) (a) Snyder, R. G. *J. Chem. Phys.* **1967**, *47*, 1316. (b) Snyder, R. G.; Schachtschneider, J. H. *Spectrochim. Acta* **1963**, *19*, 85.

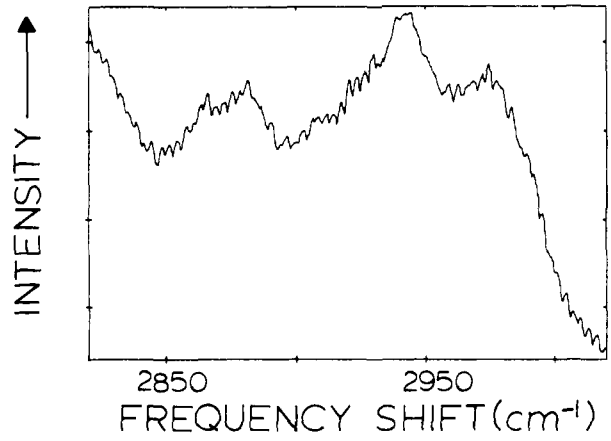


**Figure 5.** Raman spectrum of the C–H stretching region for dihexanoyl-PC 12 mM in 1 mM EDTA, 50 mM Tris solution at 22 °C. Spectral conditions: 4 scans; residence time 10 s/cm$^{-1}$; data have been seven-point smoothed.

The sensitivity of the C–H stretching region to conformational change in the alkyl chains is demonstrated for hexanoic acid in Figure 6. The most intense band in the C–H stretching regions for solid *n*-alkyl carboxylic acids arises from the antisymmetric $CH_2$ stretching modes. The band frequency decreases with increasing chain length. For example, the mode appears at 2908, 2902, and 2883 cm$^{-1}$ for solid butanoic, hexanoic, and octanoic acids, respectively.[27] As the band is expected to be rather weak in its Raman intensity, the origin of its strength has been investigated both theoretically[28] and experimentally.[27] Hill and Levin showed[27] that the same mode in *n*-octane (2881.5 cm$^{-1}$) vanishes when that solid is isolated in a $CCl_4$ matrix at low temperature. As the all-trans nature of the acyl chains is preserved at low temperature, the band therefore depends on lateral interactions between chains for its intensity. A theoretical treatment for this type of effect has been given by Snyder et al.[28] The $CH_2$ antisymmetric stretching mode intensity also is reduced when lateral interactions between hydrocarbon chains are disrupted by the formation of gauche rotamers, as occurs on melting (Figure 6). The sensitivity of this spectral feature to various types of conformational and environmental effects has resulted in this mode having been used extensively to probe lateral interactions of longer chain phospholipid molecules.[29]

Other important changes in the C–H stretching region of the *n*-hexanoic acid Raman spectrum that occur on melting include the reduction in intensity of a mode assigned to the $\alpha$-$CH_2$ stretching mode near 2923 cm$^{-1}$, and the appearance in the liquid state of a broad intense feature centered at 2919 cm$^{-1}$. The latter band is assigned to an antisymmetric $CH_2$ stretching motion which is normally only IR active, but which gains intensity in the Raman spectrum due to breakdown of selection rules in the liquid state. The apparent intensity enhancement of the $CH_3$ symmetric and antisymmetric stretching modes near 2936 and 2960 cm$^{-1}$ in the spectrum of the liquid is probably the result of increased intensity underlying these modes and originates in the broad feature at 2919 cm$^{-1}$.

The spectrum of dihexanoyl-PC will be discussed based on the data for *n*-hexanoic acid. The spectrum of the phospholipid in solid $CDCl_3$ (lipid structure unknown) shows the presence of a reasonably intense $CH_2$ antisymmetric stretching mode at 2903 cm$^{-1}$ (Figure 4B), but lacks the $\alpha$-$CH_2$ antisymmetric stretching mode at 2923 cm$^{-1}$. At room temperature, in $CDCl_3$ solution (phospholipid monomers or inverted micelles), the medium-intensity band at 2903 cm$^{-1}$ is replaced by a weak broad feature at 2907 cm$^{-1}$. In addition, a broad shoulder appears near 2921 cm$^{-1}$ characteristic of the IR-active $CH_2$ antisymmetric stretch.

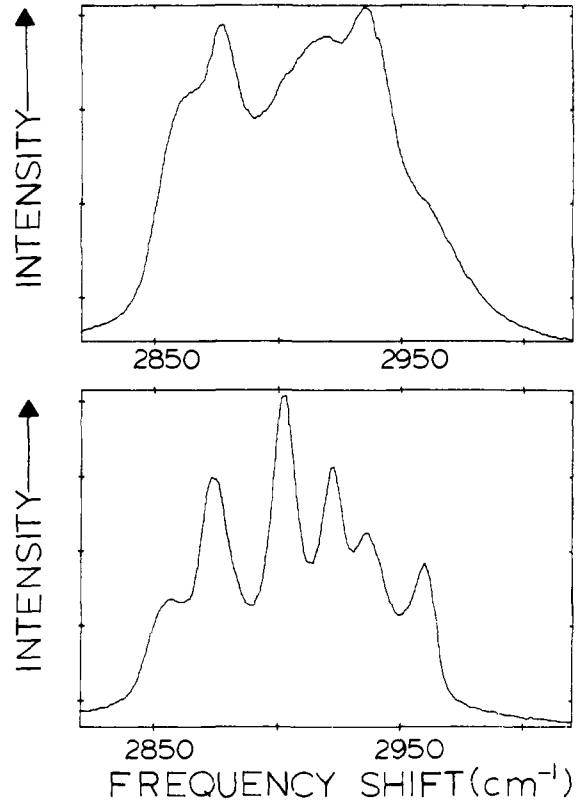


**Figure 6.** Raman spectra of the C–H stretching region for neat hexanoic acid: (i, top) 22 °C; (ii, bottom) −47 °C. Spectral conditions: single scan; spectra have not been smoothed. Other parameters as in the Experimental Section.

These observations are consistent with the elimination of extensive all-trans structure on warming from −100 °C to room temperature and are strongly suggestive of disordered hydrocarbon chains in $CDCl_3$ solutions of dihexanoyl-PC at room temperature. The residual weak band at 2907 cm$^{-1}$ in the 22 °C spectrum (Figure 4B) may reflect some remaining small population of highly interacting trans segments of $CH_2$ groups.

The spectra of dihexanoyl-PC in aqueous micelles at 22 °C and in ice (phospholipid structure unknown) are shown in Figure 4A. In addition, a spectrum of the monomer in aqueous solution is shown in Figure 5. The poor spectral quality of the latter arises from the relatively low concentration necessary to ensure monomer formation. At room temperature, the aqueous micelle has a Raman spectrum which strongly resembles that for the $CDCl_3$ solution (compare Figures 4A and 4B). The frequency differences are within experimental error with the exception of the symmetric methyl stretching mode (2941 cm$^{-1}$ in the micelle vs. 2937 cm$^{-1}$ in $CDCl_3$) and the methyl region above 2960 cm$^{-1}$. The breadth of the latter bands makes accurate frequency measurements difficult and the fact that both the terminal methyls as well as the choline methyl groups contribute to this spectral region makes it impossible for specific structural conclusions to be drawn. The acyl chain conformation (as reflected in bands at 2864, 2880, 2907, and 2920 cm$^{-1}$) is similar in the aqueous micelle and $CDCl_3$ solution states of dihexanoyl-PC. The acyl chains are significantly disordered, with perhaps a small amount of interacting trans segments still present. Very few trans-trans-trans conformations are retained, as shown by the absence of a strong antisymmetric $CH_2$ stretching mode. When the aqueous micelle is frozen in ice, the re-establishment of all-trans structure and/or strong interchain interactions is reflected in the Raman spectrum at −25 °C by the growth of a band near 2906 cm$^{-1}$ (Figure 4A).

A comparison of the spectrum of aqueous monomeric dihexanoyl-PC (Figure 5) with that of the micelle shows some significant differences in the $CH_3$ symmetric stretching mode. The frequency of the mode shows a progressive shift from 2935 cm$^{-1}$ (liquid hexanoic acid) to 2937 cm$^{-1}$ ($CDCl_3$ solution) to 2941 cm$^{-1}$

(27) Hill, I. R.; Levin, I. W. *J. Chem. Phys.* **1979**, *70*, 842.
(28) Snyder, R. G.; Hsu, S. L.; Krimm, S. *Spectrochim. Acta, Part A* **1978**, *34A*, 395.
(29) Taraschi, T.; Mendelsohn, R. *Proc. Natl. Acad. Sci. U.S.A.* **1980**, *77*, 2362.

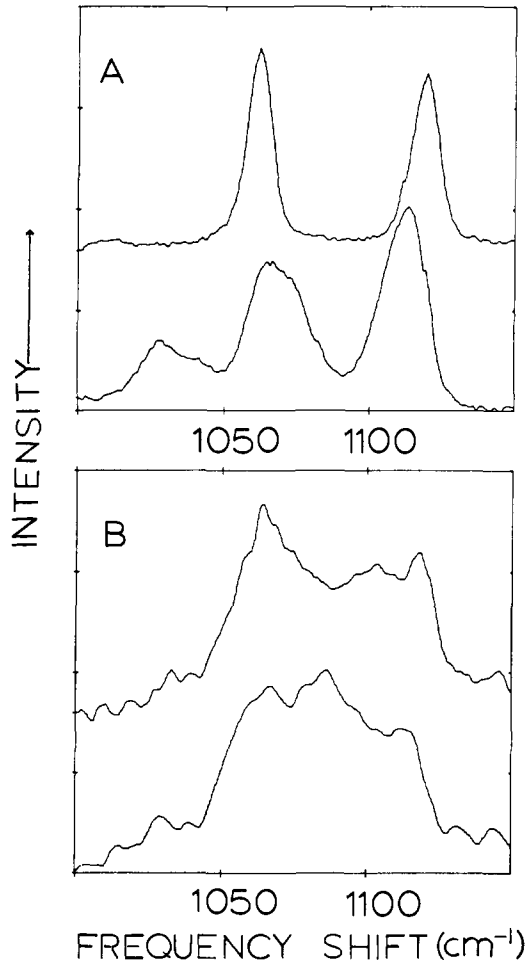


**Figure 7.** (A) Raman spectra of the C–C stretching region for neat hexanoic acid: (i, top) 22 °C (liquid); (ii, bottom) −47 °C (polycrystalline). Spectral conditions: as in Figure 4. (B) Raman spectra of the C–C stretching region for dihexanoyl-PC in (i, top) aqueous micelle (168 mM) in 1 mM EDTA, 50 mM Tris at 22 °C and (ii, bottom) micelle frozen in ice. Spectral conditions: as in Figure 4.

(aqueous micelle) to 2945 $cm^{-1}$ (aqueous monomer). This progressive increase in frequency with solvent polarity increase is similar to a trend observed in a recent Fourier transform infrared study of the monomer-to-micelle transition in sodium hexanoate.[30] For a fixed chain conformation, the relative intensity of this mode is not a strong function of solvent polarity. Its frequency appears to be a more useful indicator of the hydrocarbon chain environment. An additional difference between the aqueous monomer and the aqueous micelle is reflected in the intensity of the feature near 2907 $cm^{-1}$. The band in the monomer is so weak as to be only marginally identifiable. If the assignment of this feature to residual ordered structure in the micelle is correct, it would appear that these structures occur less frequency in the monomer in aqueous solution compared with the micelle. This observation is consistent with the $^{13}C$ NMR data (vide supra) suggestive of slightly increased numbers of trans conformers in the micelle in water compared with the monomer (in methanol). Further Raman evidence for this interpretation comes from the more pronounced shoulder near 2920 $cm^{-1}$ in the monomer than in the micelle, suggestive of more disorder in the former.

The second spectral region that has been used for monitoring structural alterations in phospholipid hydrocarbon chains is the C–C stretching region, 1000–1150 $cm^{-1}$.[31] For *n*-hexanoic acid (Figure 7A), the band in the solid near 1120 $cm^{-1}$ reflects C–C stretching modes coupled with similar modes down the length of the hydrocarbon chain. In more technical terms, the allowed Raman-active vibrations for the all-trans chain are those with identical nuclear displacements in each unit cell. If $\phi$ = the relative phase angle between adjacent units, only modes with $\phi = 0$ can appear in the spectrum of an ordered chain. Upon the introduction of gauche rotamers, C–C modes with other (fixed) values of $\phi$ become allowed.[31] For sufficiently long chains, vibrational bands with significant intensity appear at new frequencies. For *n*-hexanoic acid, these new features appear at frequencies sufficiently close to 1120 $cm^{-1}$ so that rather than a new spectral feature occurring, an apparent frequency shift is noted in the 1120-$cm^{-1}$ mode. The C–C stretching mode for hexanoic acid in the liquid state appears at 1114 $cm^{-1}$ (Figure 7A). The spectrum of dihexanoyl-PC in the C–C stretching region is shown in Figure 7B. At low temperature (micelle frozen in ice), the all-trans band appears at 1117 $cm^{-1}$. The spectral feature at 1103 $cm^{-1}$ has no counterpart in the spectrum of the *n*-hexanoic acid. There is some evidence for a symmetric stretching mode of the phosphate group at this frequency.[32] In the aqueous micelle at 22 °C, the 1117-$cm^{-1}$ mode has broadened and shifted down to 1112 $cm^{-1}$. This is the behavior expected for the introduction of modes with phase angle $\phi \neq 0$, as discussed above and in ref 31. The micelle therefore has suffered the introduction of significant numbers of gauche rotamers in its hydrocarbon chains and exhibits surprising disorder. The origin of the intense feature near 1086 $cm^{-1}$ in the micelle at 22 °C probably originates in the phosphate group. This band which appears at 1103 $cm^{-1}$ in the micelle frozen in ice appears to react to the change in hydrogen bonding experienced by the phosphate group in water compared with ice.

## Discussion

Careful analysis of the monomer/micelle transition of dihexanoyl-PC yields information relevant to several topics. Phospholipid structure is critical to the activity of a variety of enzymes, one series being the water-soluble phospholipases.[33] These esterases show markedly accelerated hydrolysis rates toward micellar or aggregated lipid compared to monomeric lipid. This enzymatic behavior has been documented with synthetic short-chain lecithins. The "interfacial activation" of the enzymes could be due in part to structural changes in the lipid molecule which occur upon aggregation. Such changes can be evaluated by physical studies of short-chain lecthins as monomers and micelles. On a more fundamental level, the structure and dynamics of micellar aggregates is currently a topic of active research.[34] In addition, this system offers a unique opportunity to study $^{13}C$ NMR chemical shift mechanisms and the factors in aggregated systems which influence Raman spectral characteristics.

Previous $^{1}H$-NMR studies of dihexanoyl-PC have shown an enhanced magnetic nonequivalence upon aggregation of the dihexanoyl-PC[35] and slight changes in rotamer population in favor of packing the two chains together. Because all carbons in the molecule are resolved $^{13}C$ NMR studies are potentially quite informative.[5,36] Upon micellization, motional changes as monitored by $T_1$ and *sn*-1/*sn*-2 chain differences as monitored by chemical shift are detected. How these relate to detailed molecular conformation is not straightforward; however, the chain nonequivalence observed in these studies is understandable in terms of X-ray structural determinations of dimyristoyl-PC and dilauroyl-DL-PE.[37] In both of these structures, the *sn*-1 and *sn*-2 chains are perpendicular and parallel, respectively, to the bilayer plane.

(30) Umemura, J.; Cameron, D. G.; Mantsch, H. H. *J. Phys. Chem.* **1980**, *84*, 2272.
(31) Lippert, J. L.; Peticolas, W. L. *Biochem. Biophys. Acta* **1972**, *282*, 8.
(32) Mendelsohn, R.; Sunder, S.; Bernstein, H. J. *Biochim. Biophys. Acta* **1975**, *413*, 329.
(33) (a) Verger, R.; DeHaas, G. H. *Annu. Rev. Biophys. Bioeng.* **1976**, *5*, 77. (b) DeHaas, G. H.; Slotboom, A. J.; Verheij, H. M. In "Cholesterol *Metabolism* and Lipolytic Enzymes", Polonovski, J., Ed.; Mason Publishing: New York, 1977; pp 191–211.
(34) Menger, F. M. *Acc. Chem. Res.* **1979**, *12*, 111.
(35) Roberts, M. F.; Bothner-By, A. A.; Dennis, E. A. *Biochemistry* **1978**, *17*, 935.
(36) Burns, R. A., Jr.; Roberts, M. F. *J. Biol. Chem.* **1981**, *256*, 2716.
(37) (a) Pearson, R. H.; Pascher, I. *Nature (London)* **1979**, *281*, 499. (b) Elder, M.; Hitchcock, P.; Mason, R.; Shipley, G. G. *Proc. R. Soc. London, Ser. A* **1977**, *354*, 157.

Analysis of solvent transfer chemical shift differences for dihexanoyl-PC indicates that the monomer/micelle transition can be successfully modeled for the majority of head-group and backbone $^{13}C$ peaks as a transfer from an H-bond-donating to an H-bond-deficient environment. No conformational changes are required to explain the $^{13}C$ chemical shift differences observed at these centers. However, the shift direction observed for the CHO backbone peak is completely inconsistent with this model, and the observed shift differences for the carbonyl resonances are grossly underestimated. We propose a conformational change between monomer and micelle for the glyceryl backbone to explain these data. These conclusions are consistent with previous $^1H$ coupling analyses of dihexanoyl-PC in a variety of physical states:[38] lipid conformation is predominantly determined by intramolecular interactions. No large changes are observed for monomeric or micellar dihexanoyl-PC in $D_2O$, or in several organic solvents. However, small differences in vicinal $^1H$ coupling constants suggested different fractional populations of glyceryl backbone torsional angles between monomeric and micellar lecithin. From the backbone and carbonyl carbon atoms affected in the monomer/micelle transition, this conformational change apparently involves some motion of the ester end of the *sn*-2 acyl chain.

The solvent transfer chemical shift differences significantly underestimate the shift difference observed for the acyl chain carbon atoms. The temperature dependence of the $^{13}C$ chemical shifts and numerous earlier studies[17b,18a,20,21] support a conformationally induced $\gamma$ effect as the additional chemical shift mechanism. Using a 5 ppm $\gamma$ effect, and correcting for a solvent effect using the well-behaved solvent-transfer data gives a $\Delta P_t$ (increase in probability of a trans conformation in the micelle) of approximately 6%. Carbon atoms 3 and 5 were used for this calculation, with carbon atom number 4 excluded; no precedent (or theoretical basis) exists for interpreting $\gamma$ effects between methylene and carbonyl groups. These data translate to $\Delta P_t$'s of 0.10 (if carbon atom number 4 is used), 0.07, and 0.05 for carbon–carbon bonds which are 2, 3, and 4 bonds from the ester carbonyl, respectively. Thus the change in chain conformation appears greater at the ester end of the chain than at the terminal methyl end. This conclusion is quantitatively supported by the intensity differences for Raman bands at 2907 and 2920 $cm^{-1}$, suggesting more chain disorder for monomeric than micellar dihexanoyl-PC. While the terminal methyl group shows a monomer/micelle $^{13}C$ chemical shift change similar to that observed for the chain methylenes, the solvent transfer data suggest that this shift change is dominated by a solvent effect. In the Raman studies, the $CH_3$ symmetric stretching mode is also shown to be dependent on solvent polarity.

$^{13}C$ NMR studies of the monomer/micelle transition of sodium octanoate[39] and *n*-nonylammonium bromide[11] demonstrate a maximum shift change in the center of the chain. Shift changes observed in that study range up to 1.2 ppm. This larger $^{13}C$ shift change upon micellization may be due to the length of these chains; $\gamma$ interactions are possible from either direction in the chain for carbon atoms in the center. The chemical shift changes in that study form a smooth distribution, although certain carbon atoms are supposedly experiencing $\gamma$ interactions with carboxylates or the ammonium moiety. This is in agreement with the results of this study, where a smooth curve can be drawn through the shift changes observed for the transition (see Figure 3A), although carbon atom number 4 has an ester carbonyl in the $\gamma$ position. Indeed, in a variety of other systems, such as 2,4,6-trichloroheptane[7b] and heteroatom-substituted ring systems,[40] the shift data are consistent with a 3–5 ppm $\gamma$ effect between methylene groups and heteroatoms. In this study, the chemical shift differences for chain carbon number 4 are similar for both ester and ether lecithins (Table I), although a carbonyl and ether methylene, respectively, are the $\gamma$ carbon atom for this center. Although the mechanisms of conformation induced chemical shifts are not well understood,[41] a variety of evidence does support the 5-ppm $\gamma$ shift in saturated chain molecules.

Interesting results are obtained if the $^{13}C$ chemical shift changes for the monomer/micelle transition are compared to the corresponding $^1H$ NMR values determined previously.[14] If the $^{13}C$ shift change is divided by the $^1H$ change for each peak, then head-group, backbone (excluding the $CH_2O$), and chain carbon 2 ratios are near zero (average = 3 (4)). Previous studies of solvent effects for cyclohexane and chloroform[6] similarly find values of this ratio near zero. In contrast, the ratios for the backbone $CH_2O$ and chain carbon 3–6 are all greater than ±30. (The backbone $CH_2O$, as in the monomer/micelle transition and the $^{13}C$ temperature dependence, appears to be involved in acyl chain conformational events.) These large values of the shift change ratio are found for carbon atoms where conformational shift mechanisms are apparently operative. Analysis of both $^{13}C$ and $^1H$ NMR shift changes (where possible) may be a fruitful approach for conformational analysis. In addition, theoretical understanding of the $\gamma$ effect $^{13}C$ shift mechanism may be gained by simultaneous analysis of the NMR shift characteristics from these two nuclei.

While NMR spectroscopy is a prominent and informative technique in studying micelles, Raman spectroscopy has been exploited to a lesser degree. The current work, along with a previous study of sodium and potassium *n*-alkyl carboxylates,[42] demonstrates both the advantages and the drawbacks of Raman spectroscopy as applied to the analysis of acyl chain structure in micellar systems. The two primary advantages are: (i) sufficient sensitivity to obtain spectra from the monomer form directly (in the current work, at a concentration of 12 mM) without the introduction of new solvent systems; and (ii) different regions of the Raman spectrum respond to different aspects of alkyl chain structure and environment. In this study, the C–C stretching modes near 1120 $cm^{-1}$ respond in frequency and intensity to the formation of gauche rotamers in the acyl chains, while the $CH_2$ antisymmetric stretching mode monitors both the lateral interactions of the hydrocarbon region as well as structural order. Finally, the terminal methyl group symmetric stretching mode frequency is a useful monitor of the solvent environment of the acyl chains.

A significant drawback in the current state of Raman spectroscopic knowledge is the lack of quantitative theories of spectra–structure relationships. Although particular vibrational modes such as the terminal methyl or phosphate vibrations may be localized on certain regions of the phospholipid, the acyl chain modes are extensively delocalized and reflect an "average" structure over all chain positions. In order to monitor specific chain positions, particular deuterated derivatives must be prepared. The C-D stretching modes can then be used to probe chain order. Another type of solution to the problem has recently been suggested.[43] Pink et al. have combined a statistical theory of chain conformation and compared it to the intensity of the C–C stretching mode. A comparison of the theoretical prediction with the observed Raman melting curves for longer chain (C-14, C-16, C-18) phosphatidylcholines gave good agreement. It may be possible in the future to go directly from the Raman intensity to a fairly accurate measure of the average number of gauche rotamers in the chain. Application of such a theory would give an independent estimate of $\Delta P_t$ for the monomer/micelle transition of dihexanoyl-PC.

The final picture of the fluid, disordered lecithin molecule in the micelle is helpful in unraveling the interfacial activation of phospholipases. The alkyl chain constraints upon aggregation are relatively minor and cannot be energetically critical to these enzymes. The conformational change in the backbone which we

(38) Hauser, H.; Guyer, W.; Pascher, I.; Skrabal, P.; Sundell, S. *Biochemistry* **1980**, *19*, 366.
(39) Drakenberg, T.; Lindman, B. *J. Colloid Interface Sci.* **1973**, *44*, 184.
(40) Eliel, E. L.; Bailey, W. F.; Kopp, L. D.; Willer, R. L.; Grant, D. M.; Bertrand, R.; Christensen, K. A.; Dalling, D. K.; Duch, M. W.; Wenkert, E.; Schell, F. M.; Cochran, D. W. *J. Am. Chem. Soc.* **1975**, *97*, 322.
(41) Levy, G. C.; Lichter, R. L.; Nelson, G. L. "Carbon-13 Nuclear Magnetic Resonance Spectroscopy", 2nd edition; Wiley-Interscience, New York, NY, 1980; p 55.
(42) Okabayshi, H.; Okuyama, M.; Kitagawa, T. *Bull. Chem. Soc. Jpn.* **1975**, *48*, 2264.
(43) Pink, D. A.; Green, T. J.; Chapman, D. *Biochemistry* **1980**, *19*, 349.

may detect cannot be discounted so easily, but it needs further definition. We are left with the possibilities that aggregation from monomer to micelle (i) alters the polarity of microenvironment of the ester groups, perhaps rendering them more susceptible to attack by phospholipases, and (ii) produces an interface with surface characteristics such as surface charge, counterion binding, etc., which alter enzyme catalysis. While the outcome of this study does not explain interfacial activation, it at least allows us to eliminate major conformational changes and ordering of the lecithin molecules as the culprits. It also provides background for further detailed studies with the enzymes.

**Acknowledgment.** We would like to thank Dr. George Benedek and Mr. Paul Missel for preliminary quasielastic light-scattering data for the size/concentration dependence of dihexanoyl-PC. The NMR experiments were performed at the NMR facility for Biomolecular Research located at the Francis Bitter National Magnet Laboratory, Massachusetts Institute of Technology (N.I.H. Grant RR00995 and N.S.F. Contract C-670), and at the Southern New England High-Field NMR facility located at Yale University. M.F.R. gratefully acknowledges support from N.S.F. PCM 7912622 and Whitaker Health Science Fund, M.I.T. R.A.B. is supported by a Whitaker Health Sciences Predoctoral Fellowship.

**Registry No.** Hexanoic acid, 142-62-1.

# Studies of Phosphorus(III) Ligands and Their Complexes of Ni(II), Pd(II), and Pt(II) Immobilized on Insoluble Supports by High-Resolution Solid-State $^{31}P$ NMR Using Magic-Angle Spinning Techniques

**L. Bemi, H. C. Clark, J. A. Davies, C. A. Fyfe,* and R. E. Wasylishen[1]**

*Contribution from The Guelph-Waterloo Centre for Graduate Work in Chemistry, Guelph Campus, University of Guelph, Guelph, Ontario N1G 2W1, Canada.*
*Received December 16, 1980*

**Abstract:** High-power proton decoupling, cross-polarization, and magic-angle spinning techniques have been employed to obtain high-resolution $^{31}P$ NMR spectra of solid tertiary phosphines, tertiary phosphine oxides, and tertiary phosphine complexes of nickel(II), palladium(II), and platinum(II). Solid-state effects can result in nonequivalence of $^{31}P$ shieldings in simple *cis*-$[PtCl_2(PR_3)_2]$ complexes. The magnitudes of the scalar couplings, $^1J(^{195}Pt,^{31}P)$, in platinum(II) complexes are comparable with those obtained by high-resolution solution $^{31}P$ NMR measurements, allowing the geometry of such complexes to be determined in the solid state. The ligand $Ph_2PCH_2CH_2Si(OEt)_3$ and its Ni(II), Pd(II), and Pt(II) complexes have been immobilized on silica gel and high-surface-area glass beads and the immobilized species studied by solid-state $^{31}P$ NMR. The results show that the geometry of surface-immobilized complexes may be determined and the surface reactions may be monitored. The merits of some preparative routes to supported transition-metal catalysts have been studied and some common representations of surface reactions and surface-immobilized species shown to be misleading.

The immobilization of transition-metal complexes on insoluble supports has been extensively studied in recent years as a method of combining the most desirable characteristics of homogeneous and heterogeneous catalysts.[2,3] Systematic research efforts in this field have been severely restricted because of the lack of suitable analytical techniques for the study and structural characterization of surface-immobilized species. The most widely utilized technique has been infrared spectroscopy,[4-6] which provides structural information in the case of immobilized species with characteristic infrared absorptions (e.g., $\nu$(CO) in metal carbonyls, $\nu$(M-H) in metal hydrides). Less commonly, electron-spin resonance,[7,8] ESCA,[9,10] photoacoustic spectroscopy,[11] and electron-probe microanalysis[12] have been utilized in attempts to obtain structural information about supported transition-metal complexes. A great many surface-immobilized complexes contain phosphorus(III) donor ligands,[2,3] but the solid-phase nature of the supported species has prevented any study by high-resolution $^{31}P$ NMR, the technique of choice when studying many homogeneous systems in solution.[13]

In recent years, the development of high-power decoupling,[14] cross-polarization,[15] and magic-angle spinning[16] techniques has allowed "high-resolution" NMR studies of dilute nuclei to be performed on solid samples. These techniques have allowed extensive study by $^{13}C$ NMR, and more recently $^{29}Si$ NMR, to be performed in many diverse areas of solid-state chemistry, including the study of surface-attached species.[17-21] The application of these techniques to the observation of the $^{31}P$ nucleus ($I = {}^1/_2$, abundance = 100%) in the solid state has recently been described in studies of the phosphate-containing phases of bones[22] and of solid

(1) On sabbatical leave from the University of Winnipeg, Department of Chemistry.
(2) (a) Hartley, F. R.; Vesey, P. N. *Adv. Organomet. Chem.* **1977**, *15*, 189. (b) Scurrell, M. S., Catalysis (London) **1978**, *2*, 215.
(3) Collman, J. P.; Hegedus, L. S. "Principles and Applications of Organotransition Metal Chemistry"; University Science Books: California, 1980; p 370.
(4) Bonds, W. D., Jr.; Brubaker, C. H., Jr.; Chandrasekaran, E. S.; Gibbons, C.; Grubbs, R. H.; Kroll, L. C. *J. Am. Chem. Soc.* **1975**, *97*, 2128.
(5) Jarrell, M. S.; Gates, B. C. *J. Catal.* **1975**, *40*, 255.
(6) Kim, T. H.; Rase, H. F. *Ind. Eng. Chem. Prod. Res. Dev.* **1976**, *15*, 249.
(7) Rollman, L. D. *J. Am. Chem. Soc.* **1975**, *97*, 2132.
(8) Bonds, W. D., Jr.; Brubaker, C. H., Jr.; Chandrasekaran, E. S.; Gibbons, C.; Grubbs, R. H.; Kroll, L. D. *J. Am. Chem. Soc.* **1975**, *97*, 2128.
(9) Takahashi, N.; Okura, I.; Keii, T. *J. Am. Chem. Soc.* **1975**, *97*, 7489.
(10) Kim, T. H.; Rase, H. F. *Ind. Eng. Chem. Prod. Res. Dev.* **1976**, *15*, 249.
(11) Somoano, R.; Gupta, A.; Volksen, W.; Rembaum, A. Coat. Plat. Prepr. *Pap. Meet. (Am. Chem. Soc., Div. Org. Cont. Plast. Chem.)* **1977**, *37*, 316.
(12) Grubbs, R. H.; Sweet, E. M. *Macromolecules* **1975**, *8*, 241.
(13) Pregosin, P. S.; Kunz, R. W. *NMR: Basic Princ. Prog.* **1979**, *16*, 1.
(14) Schaefer, J.; Stejskal, E. O. *J. Am Chem. Soc.* **1976**, *98*, 1031.
(15) Pines, A.; Gibby, M. G.; Waugh, J. S. *J. Chem. Phys.* **1972**, *56*, 1776; **1973**, *59*, 569.
(16) Andrew, E. R. *Prog. Nucl. Magn. Reson. Spectrosc.*, **1971**, *8*, 1.
(17) Chang, J. J.; Pines, A.; Fripat, J. J.; Resing, H. *Surf. Sci.* **1975**, *47*, 661.
(18) Maciel, G. E.; Sindorf, D. W. *J. Am. Chem. Soc.* **1980**, *102*, 7606.
(19) Fyfe, C. A.; Lyerla, J. R.; Yannoni, C. S. *J. Am. Chem. Soc.* **1979**, *101*, 1351.
(20) Lyerla, J. R.; Yannoni, C. S.; Bruck, D.; Fyfe, C. A. *J. Am. Chem. Soc.* **1979**, *101*, 4770.
(21) Shiau, W.-I.; Duesler, E. N.; Paul, I. C.; Blann, W. G.; Fyfe, C. A. *J. Am. Chem. Soc.* **1980**, *102*, 4546.

0002-7863/82/1504-0438$01.25/0 